Journal of Alloys and Compounds, 197 (1993) 145–152
JALCOM 7314

Structural stability, local topology and electron count in small s-valent clusters

Mehul Shah and D. G. Pettifor*
Department of Mathematics, Imperial College of Science, Technology and Medicine, London SW7 2BZ (UK)

Abstract

The relative stability of three-, four-, five- and six-atom s-valent clusters has been investigated within a nearest-neighbour tight-binding Hückel model. The predicted structural trends as a function of electron count are related directly to the cluster topology by using the ring approximation to the bond order. The importance of cluster connectivity rather than symmetry is stressed.

1. Introduction

Recently the use of local coordination polyhedra has been shown to provide a simplying classification of elemental, binary and ternary structure types [1–3]. It has been found, for example, that 95% of all reported elemental structural modifications can be classified with just seven different local coordination polyhedra or atomic environment types [3], whereas 92% of the local atomic environments found in cubic intermetallic structure types can be described by only 21 different local coordination polyhedra [2]. It is therefore very important for structural prediction to understand the factors determining the choice of atomic environment type and hence the possible structure types.

The study of the stability of small clusters is an ideal area for examining the factors which control structural stability, since clusters have the ability to take many different atomic configurations owing to the lack of the constraint of long-range periodicity (see *e.g.* Table 1 of ref. 4). During the past few years there has been much progress in the first-principles prediction of cluster stability. Here, however, we will use the simplest possible nearest-neighbour tight-binding (TB) Hückel model in order to demonstrate the close link between structural stability, local topology and electron count. This close link has already been stressed by numerous authors (see refs. 5–9 and references cited therein). We will make the connection more transparent for s-valent systems by using the recently proposed ring approximation for the bond order [10, 11].

*Author to whom correspondence should be addressed. Present address: Department of Materials, University of Oxford, Parks Road, Oxford OX1 3PH, UK.

The outline of the paper is as follows. In Section 2 we present the nearest-neighbour TB Hückel model for describing the energetics of s-valent clusters. The structural energy difference theorem [12] is introduced, thereby allowing a direct prediction of the relative stabilities of different symmetric clusters in terms of the bond energy alone. In Section 3 the predicted structural trends are interpreted in terms of the local topology about the bond by using the ring approximation for the bond order. In Section 4 we conclude.

2. The TB Hückel model

The binding energy per atom for a cluster of $\mathcal{N}$ s-valent atoms may be written in the form [13, 14]

$$U = U_{\text{rep}} + U_{\text{bond}} \tag{1}$$

where U_{rep} is a semiempirical pairwise repulsive contribution, namely

$$U_{\text{rep}} = \frac{1}{2\mathcal{N}} \sum_{i,j}{}' \Phi(R_{ij}) \tag{2}$$

and U_{bond} is the attractive covalent bond energy, namely

$$U_{\text{bond}} = \frac{1}{\mathcal{N}} \sum_n f_n \epsilon_n \tag{3}$$

with f_n the electron occupancy of the eigenvalue ϵ_n. For the symmetric clusters considered in this paper the eigenvalues are obtained by solving the nearest-neighbour orthogonal TB secular equation

$$|H - \epsilon I| = 0 \tag{4}$$

0925-8388/93/$6.00

where I is the unit matrix. The hamiltonian matrix H has zero elements everywhere except between nearest-neighbour sites i and j when $H_{ij} = -h_c$, where c labels the particular cluster geometry. Note that H_{ij} is negative since it corresponds to the overlap of two s-orbitals in a negative potential; h_c is therefore a positive quantity.

Figure 1 shows the resultant eigenspectra of different symmetric clusters with up to six atoms, the energy scale of each cluster being set by the appropriate value of h_c. The clusters include the most stable ground state geometries of neutral and singly ionized systems which were found by Wang *et al.* [4] in their global search over *all* geometries constrained by the same nearest-neighbour distance. We have ordered the cluster geometries in Fig. 1 from left to right according to whether they are three dimensional, two dimensional or one dimensional respectively. For a given dimension they are ordered from left to right according to the degree of skewness of their eigenspectrum. This is measured by the normalized third moment $\mu_3/\mu_2^{3/2}$, where the pth moment of the eigenspectrum is defined by

$$\mu_p = \sum_n \epsilon_n^p \tag{5}$$

For three-atom clusters the triangle and linear chain have a skewness of -0.41 and 0 respectively. For four-atom clusters the tetrahedron, rhombus, square and linear chain have a skewness of -0.58, -0.38, 0 and 0 respectively. For five-atom clusters the trigonal bipyramid, monofinned tetrahedron, square pyramid, close-packed layer, pentagon and linear chain have a skewness of -0.55, -0.47, -0.38, -0.34, 0 and 0 respectively. For six-atom clusters the trigonal tripyramid, octahedron, pentagonal pyramid, trigonal prism, close-packed layer, hexagon and linear chain have a skewness of -0.51, -0.41, -0.34, -0.16, -0.31, 0 and 0 respectively.

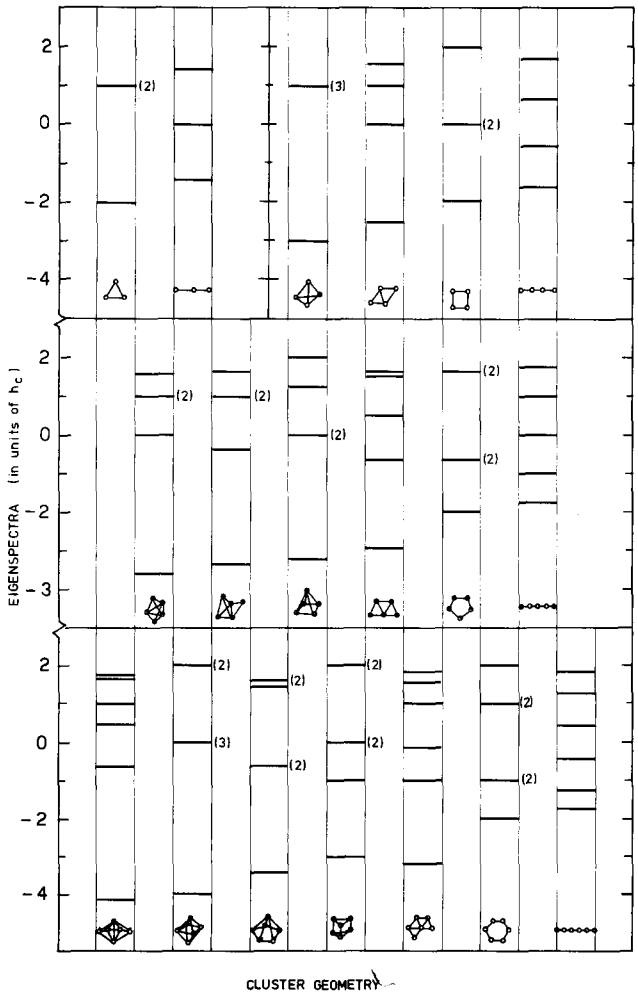

Fig. 1. Eigenspectra of three-, four-, five- and six-atom clusters in units of h_c, the magnitude of the nearest-neighbour bond integral for a given cluster. The numbers in parentheses give the degeneracy of the level.

This varying degree of skewness of the TB eigenspectra may be related directly to the topology of the clusters as first shown by Cyrot-Lackmann [15]. It follows from eqns. (4) and (5) that

$$\mu_p = \sum_n \epsilon_n^p = \sum_n (H^p)_{nn} = \mathrm{Tr}H^p \tag{6}$$

However, because the trace is invariant with respect to the choice of basis functions which are related by a unitary transformation, we may work with the basis of s-orbitals on the different atomic sites (labelled by i) rather than the basis of eigenfunctions (labelled by n). That is,

$$\mu_p = \mathrm{Tr}H^p = \sum_i (H^p)_{ii} \tag{7}$$

so that using matrix multiplication we have

$$\mu_p = \sum_{i, i_1, i_2, \ldots, i_{p-1}} H_{ii_1} H_{i_1 i_2} \ldots H_{i_{p-1} i} \tag{8}$$

Thus the *second* moment μ_2 is given by summing over all paths of length *two* from $i \to j \to i$, namely

$$\mu_2 = \sum_{i,j}{}' H_{ij} H_{ji} \tag{9}$$

whereas the *third* moment μ_3 is given by summing over all paths of length *three* from $i \to j \to k \to$ i, namely

$$\mu_3 = \sum_{ijk}{}' H_{ij} H_{jk} H_{ki} \tag{10}$$

The prime in the summation indicates that $i \neq j \neq k$, since the diagonal on-site energies H_{ii} vanish because the *bond* energy in eqn. (3) is defined with respect to these on-site energies.

The skewness is therefore related to the number of three-member rings ijk present in the cluster. Consider, for example, the pentagonal pyramid (which we will label c_1) and the trigonal prism (which we will label

c_2), both consisting of six atoms as illustrated at the bottom of Fig. 1. It follows from eqns. (9) and (10) that for the pentagonal pyramid we have

$$\mu_2^{(c1)} = (5\times 3 + 1\times 5)h_{c_1}^2 = 20h_{c_1}^2 \tag{11}$$

and

$$\mu_3^{(c1)} = -(5\times 4 + 1\times 10)h_{c_1}^3 = -30h_{c_1}^3 \tag{12}$$

so that $\mu_3/\mu_2^{3/2} = -0.34$ as noted earlier. On the other hand, for the trigonal prism we have

$$\mu_2^{(c2)} = (6\times 3)h_{c_2}^2 = 18h_{c_2}^2 \tag{13}$$

and

$$\mu_3^{(c2)} = -(6\times 2)h_{c_2}^3 = -12h_{c_2}^3 \tag{14}$$

so that $\mu_3/\mu_2^{3/2} = -0.16$ as noted earlier.

The relative structural stabilities of the different cluster geometries will be predicted by using the structural energy difference theorem [12]. This states that the difference in the total energy per atom, ΔU, between two systems in equilibrium under a binding energy law of the type given by eqn. (1) is, to first order in $\Delta U/U$,

$$\Delta U = (\Delta U_{\text{bond}})_{\Delta U_{\text{rep}}=0} \tag{15}$$

That is, the difference in the total energy per atom is simply the difference in the bond energy provided that the bond lengths have been adjusted so that the clusters have identical repulsive energies.

We will assume that the repulsive pairwise potential $\Phi(R)$ in eqn. (2) is proportional to the magnitude of the ssσ bond integral $h(R)$, namely

$$\Phi(R) \propto h^{\lambda}(R) \tag{16}$$

The index λ is therefore a measure of the steepness of the repulsive pair potential compared with that of the attractive bonding contribution. For hydrogen [16, 17] and most sp-bonded elements [6, 18, 19] $\lambda \approx 2$. For lithium Abell [17] found that the much larger value of $\lambda \approx 8$ was required in order to fit the molecular binding energy curves within an s-valent TB Hückel model. Here we will consider the three values $\lambda = 2$, 3 and ∞. The last value corresponds to an infinitely steep repulsive pair potential which implies the fixed nearest-neighbour distance taken by Wang *et al.* [4] in their cluster studies.

The structural energy difference theorem allows the nearest-neighbour bond integral h_c for any cluster c to be given in terms of the bond integral of some reference cluster. Taking the dimer as reference with bond integral h_0 and setting $\Delta U_{\text{rep}} = 0$, we have from eqns. (2) and (16) that

$$\frac{1}{\mathcal{N}} \sum_{i,j} h^{\lambda}(R_{ij}) = h_0^{\lambda} \tag{17}$$

where $h(R_{ij}) = h_c$ for nearest neighbours i and j. Thus, for example, the pentagonal pyramid will have

$$\tfrac{1}{6}(5\times 3 + 1\times 5)h_{c_1}^{\lambda} = h_0^{\lambda} \tag{18}$$

whereas the trigonal prism will have

$$\tfrac{1}{6}(6\times 3)h_{c_2}^{\lambda} = h_0^{\lambda} \tag{19}$$

i.e. $h_{c_1} = h_0/(10\times 3)^{1/\lambda}$ and $h_{c_2} = h_0/3^{1/\lambda}$. We see that for $\lambda = \infty$, $h_{c_1} = h_{c_2} = h_0$, *i.e.* the nearest-neighbour bond integral is cluster independent.

The upper panels of Figs. 2–5 show the predicted bond energies per atom for three-, four-, five- and six-atom clusters respectively as a function of the electron count N for the three different values of λ, namely $\lambda = 2$, 3 and ∞. The influence of λ on the relative stability is clearly illustrated by Fig. 2. We see that for $\lambda = \infty$, when all clusters take the same nearest-neighbour bond length and hence have identical bond integrals, the triangle is predicted to be the most stable cluster for the neutral monovalent system, whereas for $\lambda = 2$ and 3 the linear chain is the most stable. Thus whereas the alkalis take a (Jahn–Teller-distorted) triangular configuration with their large values of λ (*e.g.* $\lambda \approx 8$ for lithium [17]), hydrogen remains linear since $\lambda \approx 2$ [16, 17]. As expected, decreasing λ favours less topologically close-packed structures with lower coordination. The singly ionized cluster corresponding to $N = 2$ takes the triangular geometry for all three values of λ.

The $\lambda = \infty$ upper panel of Figs. 3–5 show that the rhombus, close-packed plane and pentagonal pyramid are the most stable geometries for the neutral four-, five- and six-atom clusters respectively, whereas the singly ionized systems take the rhombus, monofinned tetrahedron and trigonal tripyramid geometries respectively, as predicted by Wang *et al.* [4]. Again we see that a decrease in λ stabilizes lower-coordinated structures, so that for $\lambda = 2$ the most stable geometry is the linear chain for four- and five-atom neutral clusters and the hexagon for six-atom clusters.

We also see that for $\lambda = 2$ the dimer has the lowest binding energy per atom, namely -1, whereas for $\lambda = \infty$ the dimer has the highest energy of all the ground state clusters. This is consistent with hydrogen being dimeric but the alkalis being close-packed metals.

As expected from Fig. 1, the geometries with skew eigenspectra are the most stable for low electron count, whereas those with no three-member rings are the most stable for high electron count (excluding the square pyramid for $\lambda = \infty$). The link between the structural trends as a function of electron count and the topology of the cluster will be provided in the next section by the ring approximation to the bond order.

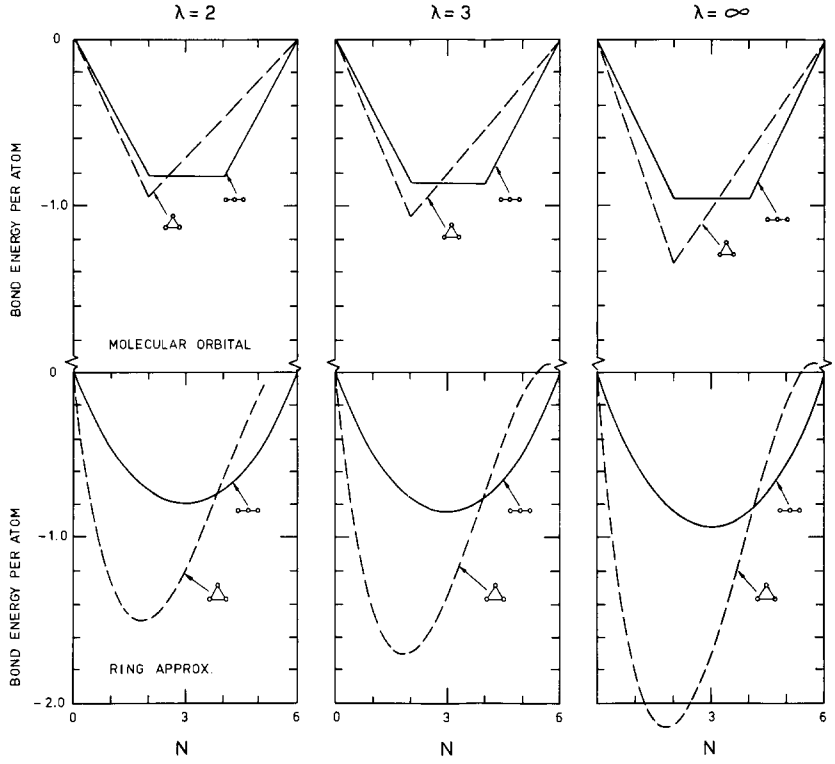

Fig. 2. Average bond energy per atom (in units of h_0) as a function of electron count N for three-atom clusters.

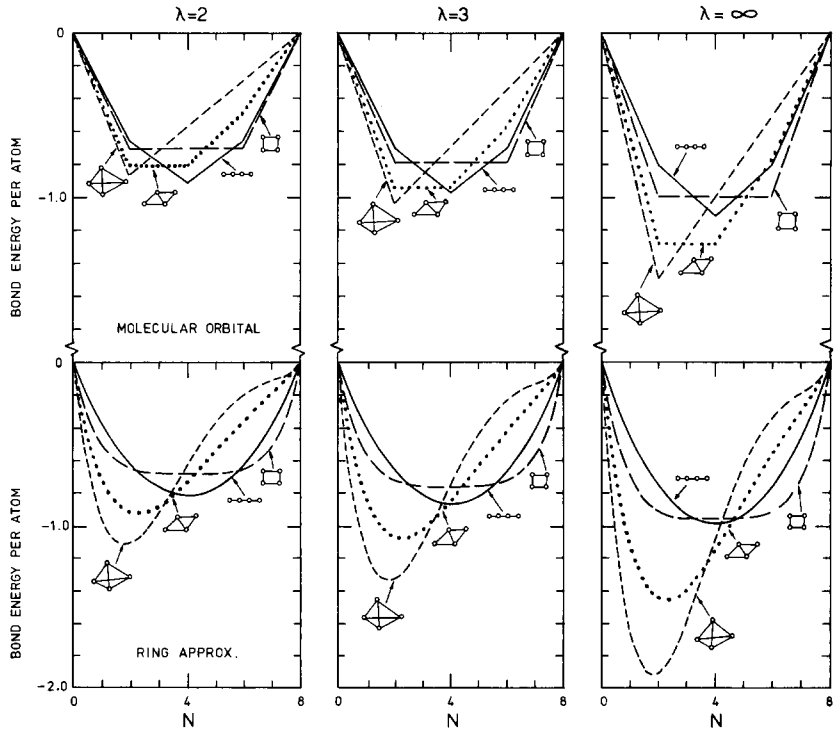

Fig. 3. Average bond energy per atom (in units of h_0) as a function of electron count N for four-atom clusters.

3. Origin of the structural trends

Although an analysis in terms of the third moment shows that the skewness of a given eigenspectrum is due to the presence of three-member rings within the cluster, in general the inclusion of higher moments leads to a notoriously ill-conditioned problem (see ref. 20 and references cited therein). Recently a many-atom

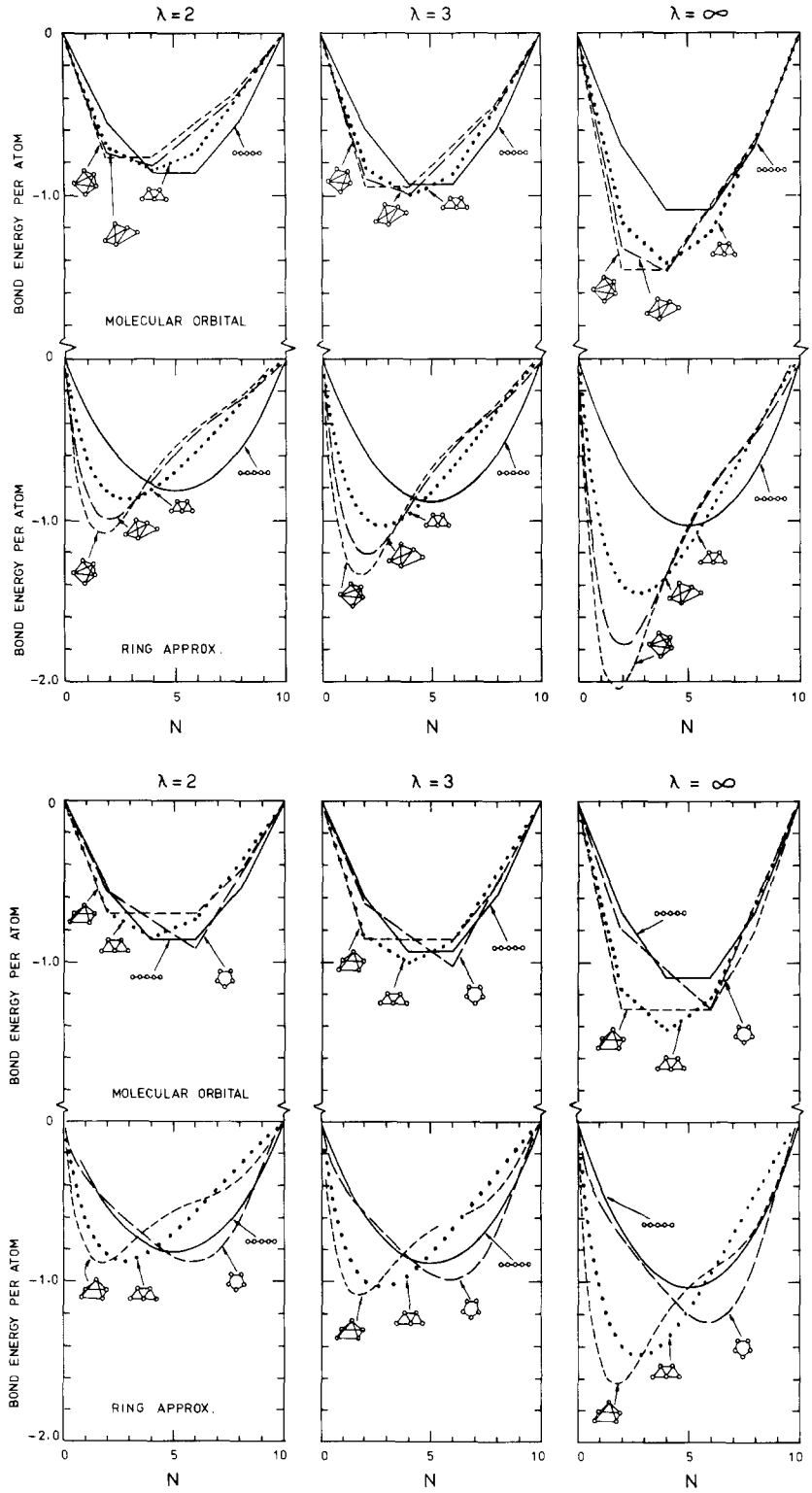

Fig. 4. Average bond energy per atom (in units of h_0) as a function of electron count N for five-atom clusters.

expansion has been derived for the bond order which is fairly rapidly convergent [21]. In order to understand the trends displayed in Figs. 2–5, we will use this expansion in its simplest form, namely within the so-called ring approximation [10, 11].

The bond energy per atom of eqn. (3) may be written explicitly as a sum over the individual bond contributions, namely

$$U_{\text{bond}} = \frac{1}{2\mathcal{N}} \sum_{i,j}{}' U^{ij}_{\text{bond}} \tag{20}$$

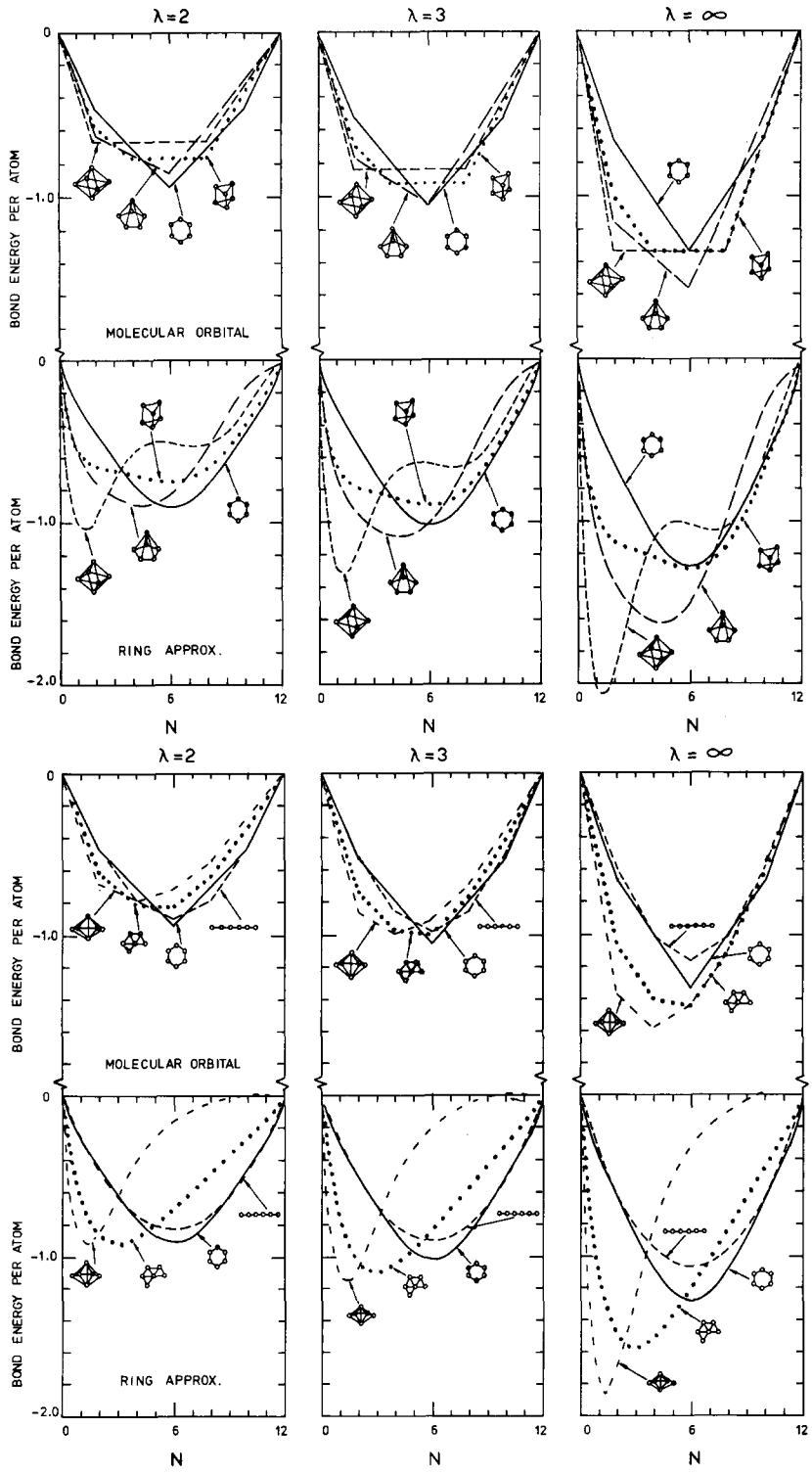

Fig. 5. Average bond energy per atom (in units of h_0) as a function of electron count N for six-atom clusters.

Following Coulson [22], the individual bond energy between atoms i and j is given by the product of the bond integral and the bond order, namely

$$U^{ij}_{\text{bond}} = -2h(R_{ij})\Theta_{ij} \tag{21}$$

where the prefactor 2 assumes spin degeneracy. (Note that there is no explicit spin-dependent exchange energy in the TB Hückel secular equation (4), so that the energy of the singly occupied eigenstate with a given spin is equivalent to the energy of the hypothetical non-magnetic state corresponding to opposite spin states

each occupied by half an electron.) The bond order Θ_{ij} is defined as the difference between the number of electrons of a given spin in the bonding, $2^{-1/2}(\psi_i+\psi_j)$, and antibonding, $2^{-1/2}(\psi_i-\psi_j)$, states. Thus the bond order is unity for the neutral dimer but is expected to be less than unity for the bonds in other clusters owing to the additional bonding with neighbouring atoms.

The dependence of the bond order on the local environment is given within the ring approximation by [10, 11]

$$\Theta_{ij}=2\sum_{n=2}^{\infty}\hat{\chi}_n\left(\frac{N}{\mathcal{N}}\right)\frac{\zeta_n^{\text{ring}}}{b^{n-1}} \tag{22}$$

The reduced susceptibility $\hat{\chi}_n$ is a function of the number of electrons (of both spins) per atom, $N/\mathcal{N}$. It is given by the analytical expression

$$\hat{\chi}_n(\phi_F)=\frac{1}{\pi}\left(\frac{\sin[(n-1)\phi_F]}{n-1}-\frac{\sin[(n+1)\phi_F]}{n+1}\right) \tag{23}$$

where ϕ_F is related to the number of electrons per atom, $N/\mathcal{N}$, through

$$\frac{N}{\mathcal{N}}=\frac{2\phi_F}{\pi}\left(1-\frac{\sin(2\phi_F)}{2\phi_F}\right) \tag{24}$$

Figure 6 shows the behaviour of the first five reduced response functions $\hat{\chi}_n$ as a function of the number of electrons per atom. We see that the number of nodes (excluding the end points) equals $n-2$. The parameter ζ_n^{ring} is given by the sum over all ring-type paths of length $n-1$ linking atoms i and j, so that the first three contributions entering eqn. (22) take the form

$$\zeta_2^{\text{ring}}=H_{ij} \tag{25}$$

$$\zeta_3^{\text{ring}}=\sum_k{}'H_{ik}H_{kj} \tag{26}$$

and

$$\zeta_4^{\text{ring}}=\sum_k{}'H_{ik}H_{kl}H_{lj} \tag{27}$$

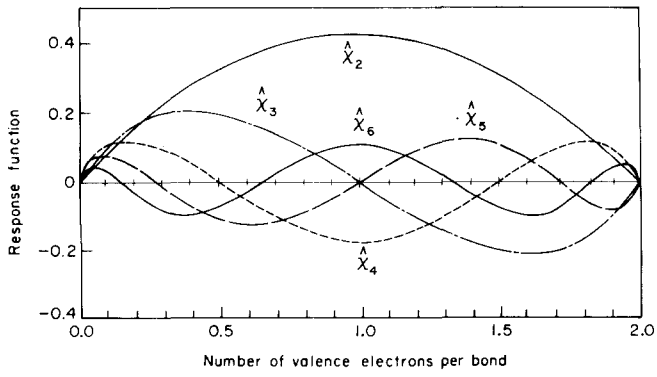

Fig. 6. Reduced response function $\hat{\chi}_n$ as a function of number of electrons per atom.

The parameter b is an embedding function which results from embedding the given bond ij in its cluster environment. It takes the second-moment form

$$b=\left[\frac{1}{2}\left(\sum_{k\neq i}H_{ik}^2+\sum_{k\neq j}H_{jk}^2\right)\right]^{1/2} \tag{28}$$

The results of this simple analytic model are shown in the lower panels of Figs. 2–5. We see that the ring approximation predicts the correct structural *trends* between different geometries with a fixed number of atoms but that it is at best qualitative with respect to the absolute energy. For quantitative predictions we must both use more accurate response functions $\hat{\chi}_n$ and include so-called double-counting terms in ζ_n (see eqns. (2.8), (2.9) and (2.20)–(2.30) of ref. 11 and Fig. 1 of ref. 21).

The structural trends may therefore be related directly to the topology of the cluster through the ring approximation of eqn. (22). Consider, for example, the four-atom clusters shown in Fig. 3. The bond energy is particularly simple to evaluate for the case where all bonds in the cluster are equivalent, such as for the square and tetrahedron. It follows from eqns. (17) and (20)–(28) that for $\lambda=2$ the average bond energy per atom for the square will be given by

$$U_{\text{bond}}^{\text{square}}=-(2\hat{\chi}_2+\hat{\chi}_4)h_0 \tag{29}$$

whereas for the tetrahedron it will be given by

$$U_{\text{bond}}^{\text{tetrahedron}}=-[2\hat{\chi}_2+(4/3^{1/2})\hat{\chi}_3+(4/3)\hat{\chi}_4]h_0 \tag{30}$$

Thus whereas the one-dimensional linear chain has only the $\hat{\chi}_2$ prefactor in its expansion for the bond order and therefore varies in a parabolic-like fashion across the lower left-hand panel of Fig. 3, the two-dimensional square has an additional $\hat{\chi}_4$ contribution (see eqn. (29)). From Fig. 6 this four-member ring contribution increases the bonding for low and high electron counts but decreases it in between, which can be seen directly by comparing the curves for the linear chain and square in Fig. 3. Folding the square along the diagonal to create the three-dimensional tetrahedron introduces three-member rings and therefore a $\hat{\chi}_3$ factor (see eqn. (30)). From Fig. 6 this skews the binding energy curves downwards for low electron count and upwards for high electron count. Distorting the square into a rhombus also introduces three-member rings, so that the curve of the rhombus is skewed compared with that of the square. Thus in Fig. 3 we see the trend for $\lambda=2$ from tetrahedron to rhombus to linear chain to square as the electron count increases.

The structural trend across the five- and six-atom clusters in Figs. 4 and 5 can be understood in a similar way in terms of the presence (or absence) of three-, four-, five- and six-member rings. In particular, the six-

member ring stabilizes the hexagon rather than the linear chain for neutral clusters in agreement with the well-known Hückel rule [8].

4. Conclusions

The relative stability of three-, four-, five- and six atom s-valent clusters has been investigated within a nearest-neighbour TB Hückel model. The use of the structural energy difference theorem has allowed their stability to be related to the sum of the one-electron eigenvalues by taking account of the appropriate change in the nearest-neighbour bond integrals with cluster geometry and coordination. The structural trends predicted by the TB Hückel model can be understood within the ring approximation: three-member rings favouring electron counts with less than half-full bonds, four-member rings stabilizing clusters with low and high electron counts and six-member rings favouring clusters with half-full bonds.

As stressed by Burdett [8], the *connectivity* of the cluster is more important in determining its binding energy than is its *symmetry*. This relates immediately to the work of Villars, Daams and others [1–4] who have found that the many thousands of different structure types, characterized by symmetry, are associated with only a relatively few important local coordination polyhedra, characterized by connectivity. It remains, however, to discover whether these local coordination polyhedra or atomic environment types can be predicted with a few simple rules.

References

1 P. Villars, K. Mathis and F. Hulliger, in F. R. de Boer and D. G. Pettifor (eds.), *The Structures of Binary Compounds*, Vol. 2, North-Holland, Amsterdam, 1989, pp. 1–102.
2 J. L. C. Daams, J. H. N. van Vucht and P. Villars, *J. Alloys Comp., 182* (1992) 1.
3 P. Villars and J. L. C. Daams, *J. Alloys Comp., 197* (1993) 177.
4 Y. Wang, T. F. George, D. M. Lindsay and A. C. Beri, *J. Chem. Phys., 86* (1987) 3493.
5 F. Ducastelle and F. Cyrot-Lackmann, *J. Phys. Chem. Solids, 32* (1971) 285.
6 J. C. Cressoni and D. G. Pettifor, *J. Phys.: Condens. Matter, 3* (1991) 495.
7 J. K. Burdett and S. Lee, *J. Am. Chem. Soc., 107* (1985) 3063.
8 J. K. Burdett, *Acc. Chem. Res., 21* (1988) 189.
9 F. Ducastelle, *Order and Phase Stability in Alloys*, North-Holland, Amsterdam, 1991.
10 D. G. Pettifor, *Phys. Rev. Lett., 63* (1989) 2480.
11 D. G. Pettifor and M. Aoki, *Philos. Trans. R. Soc. Lond. A, 334* (1991) 439.
12 D. G. Pettifor, *J. Phys. C: Solid State Phys., 19* (1986) 285.
13 F. Ducastelle, *J. Phys. (Paris), 31* (1970) 1055.
14 A. P. Sutton, M. W. Finnis, D. G. Pettifor and Y. Ohta, *J. Phys. C: Solid State Phys., 21* (1988) 35.
15 F. Cyrot-Lackmann, *Adv. Phys., 16* (1967) 393.
16 A. J. Skinner and D. G. Pettifor, *J. Phys.: Condens. Matter, 3* (1991) 2029.
17 G. C. Abell, *Phys. Rev. B, 31* (1985) 6184.
18 M. Lannoo, *J. Phys. (Paris), 40* (1979) 461.
19 L. Goodwin, A. J. Skinner and D. G. Pettifor, *Europhys. Lett., 9* (1989) 701.
20 R. Haydock, *Solid State Phys., 35* (1980) 215.
21 M. Aoki and D. G. Pettifor, *Proc. Int. Conf. on Physics of Transition Metals*, Darmstadt, July 1992.
22 C. A. Coulson, *Proc. R. Soc. A, 169* (1939) 413.